Resolving vesicle fusion from lysis to monitor calcium-triggered lysosomal exocytosis in astrocytes

Jyoti K. Jaiswal*†, Marina Fix*, Takahiro Takano‡, Maiken Nedergaard‡, and Sanford M. Simon*†

*The Rockefeller University, 1230 York Avenue, Box 304, New York, NY 10065; and ‡Center for Aging and Developmental Biology, University of Rochester Medical Center, 601 Elmwood Avenue, Rochester, NY 14642

Edited by Rodolfo R. Llinas, New York University Medical School, New York, NY, and approved July 2, 2007 (received for review May 29, 2007)

Optical imaging of individual vesicle exocytosis is providing new insights into the mechanism and regulation of secretion by cells. To study calcium-triggered secretion from astrocytes, we used acridine orange (AO) to label vesicles. Although AO is often used for imaging exocytosis, we found that imaging vesicles labeled with AO can result in their photolysis. Here, we define experimental and analytical approaches that permit us to distinguish unambiguously between fusion, leakage, and lysis of individual vesicles. We have used this approach to demonstrate that lysosomes undergo calcium-triggered exocytosis in astrocytes.

acridine orange | imaging | secretion | evanescent wave microscopy | ATP

Exocytosis, the process by which a vesicle inside of a cell fuses to the cell surface, serves a plethora of important functions in all eukaryotic cells. These include insertion of membrane proteins such as ion channels and receptors, addition of new membranes during neuronal development, and secretion of neurotransmitter at the synapse.

Over the past few decades, much has been learned about the physiology of exocytosis in neurons. Through the use of biochemistry, electrophysiology, and genetics, a considerable body of knowledge has been gathered about the molecular participants in exocytosis. However, much remains to be learned about the dynamics of these molecules. Our knowledge has been limited in part by our ability to image single molecules, or even the fusion of single vesicles. Fortunately, the use of total internal reflection fluorescence microscopy (TIR-FM) allows imaging fusion of single vesicles (1–6).

Ca^{2+}-triggered exocytosis, considered a hallmark of excitable cells, has also been reported in nonexcitable cells such as fibroblasts (5, 7–9). In all nonexcitable cells, Ca^{2+}-triggered exocytosis is believed to serve a role in membrane repair (10). Additionally, some cells, such as hematopoietic cells, use Ca^{2+}-triggered exocytosis for specialized functions such as release of cytolytic molecules (11). Astrocytes are nonexcitable cells of the nervous system that were previously thought to have only a protective role for neurons. However, astrocytes have now been shown to be more intricately involved in regulating neuronal physiology (12–14). This is believed in part to be due to the ability of astrocytes to exocytose a variety of molecules (15).

Exocytosis of synaptic vesicles (16), dense core granules (3, 17), and even astrocytic vesicles that undergo Ca^{2+}-triggered exocytosis (18) have been imaged by using the fluorescence of acridine orange (AO), a weak base that accumulates in acidified vesicles (19). Accumulation at high concentrations causes quenching of AO fluorescence. On release from the vesicle, AO fluorescence is unquenched and thus increases rapidly. Such rapid increase in AO fluorescence followed by its lateral diffusion is called an "AO flash" and has been used as a hallmark of exocytosis (3, 20–22).

To examine potential Ca^{2+}-regulated exocytic vesicles in astrocytes, we incubated the cells with AO. The basal surface of the astrocytes was then imaged by TIR-FM. Our initial observations with AO were consistent with what has been previously reported: bright flashes from the vesicles labeled with AO (3, 18, 20). However, many of our subsequent observations were inconsistent with the interpretation that AO flashes represent exocytosis of the labeled vesicles. Instead, the results were most consistent with illumination of AO-labeled vesicles inducing photolysis and rupturing of the vesicles. Here, we demonstrate a set of techniques that can be used to distinguish between vesicle lysis and fusion. These techniques allow quantification of the steps of vesicular fusion, including the delivery of membrane and luminal contents. Use of this strategy has allowed us to establish lysosomes as regulated exocytic vesicles in astrocytes. Our approach is required not only for characterizing and studying exocytosis in astrocytes but also for studying vesicle exocytosis in other cell types.

Results

At low concentrations, AO has a broad fluorescence emission with a major peak at 535 nm and a minor one at 630 nm (Fig. 1*A*). With increasing concentration, the fluorophore forms dimers (23). This causes triplet quenching of the green emission and results in red fluorescence with a peak at 630 nm (Fig. 1*A*). AO preferentially accumulates in acidic compartments, such as endosomes, lysosomes, and secretory vesicles (24). In these organelles, it can accumulate to high enough concentrations that it fluoresces red. When rat astrocytes were incubated with 0.1–5 μM AO, there was a diffuse green (515/50 bandpass emission filter) fluorescence throughout the cytosol as well as many discrete puncta with red emission (580 long-pass emission filter) (Fig. 1*B*).

Many AO-labeled vesicles were observed when the basal surface of the rat astrocyte was imaged with evanescent wave/TIR-FM (Figs. 1*B* and 2 *A* and *C*). Within 3 s of initiating imaging, we observed "AO flashes," an increase in red fluorescence followed by rapid spread and dissipation of red fluorescence (Fig. 2 *A* and *B*). During the segment shown (Fig. 2*A*), some of the vesicles (marked by the arrow) released their fluorescence and others (marked by the arrowhead) did not. However, when imaged for longer periods (3 min), all of the AO-labeled vesicles near the cell membrane released their red AO fluorescence. The lateral spread of the fluorescence was similar to what has been observed on the exocytosis of vesicles with other luminal fluorophores (5, 17, 25). Surprisingly, only the cells that were imaged [supporting information (SI) Movie 1 and SI Fig. 5] lost the fluorescence from the AO-labeled vesicles.

Author contributions: J.K.J. and S.M.S. designed research; J.K.J. and M.F. performed research; T.T. and M.N. contributed new reagents/analytic tools; J.K.J., M.F., and S.M.S. analyzed data; and J.K.J., M.F., and S.M.S. wrote the paper.

The authors declare no conflict of interest.

This article is a PNAS Direct Submission.

Abbreviations: TIR-FM, total internal reflection fluorescence microscopy; AO, acridine orange; Cer, Cerulean.

†To whom correspondence may be addressed. E-mail: jaiswaj@rockefeller.edu or simon@rockefeller.edu.

This article contains supporting information online at www.pnas.org/cgi/content/full/0704935104/DC1.

NEUROSCIENCE

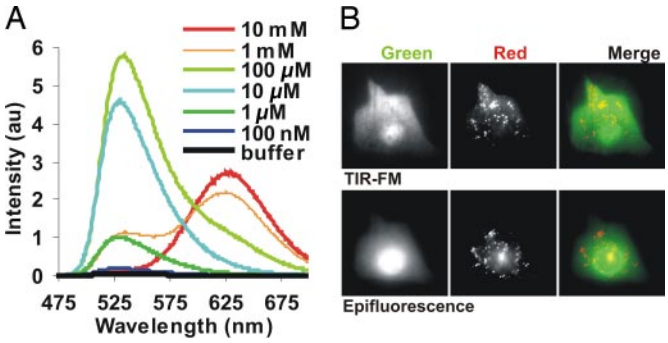

Fig. 1. Concentration-dependent change in AO spectra. (*A*) Emission spectra of AO at various concentrations in sodium acetate buffer (pH 5.0; excitation with 442-nm light). (*B*) A rat astrocyte labeled with 5 μM AO was imaged by using 488-nm laser in TIR-FM and epifluorescence mode. The images show the emission collected using 515/30 bandpass filter (green) or 580lp filter (red) and an overlay of these two images.

Cells outside the imaging area (dotted circle in SI Fig. 5 and each new field in SI Movie 1) still contained AO-labeled vesicles. However, on initiation of imaging, these vesicles also exhibited the characteristic AO flashes. When we simultaneously imaged multiple AO-labeled cells by using epifluorescence microscopy, we found that, for all of the cells, it took <5 s to detect the first release of AO (Fig. 2 *D* and *E*, arrows in the plot). The time to initiate AO release from the vesicles depended on the intensity of the excitation light. Imaging at 1-mW power with a 488-nm laser in TIR-FM illumination mode, the first release occurred after 5 s, and significant release persisted even after 30 s (Fig. 2 *E* and *F*). When 10-mW excitation power was used, release of AO from all of the labeled vesicles occurred within 10 s, with the bulk of release occurring within the first 5 s (Fig. 2*F*).

These results indicate that the release of AO from vesicles depended on illumination. This was the first observation that was not consistent with what we expected when observing Ca^{2+}-triggered exocytosis. In cells with many AO-labeled fluorescent puncta (Fig. 2*Ci*), 3 min of continuous evanescent wave illumination with 1 mW of a 488-nm laser caused all vesicles to release their AO content, leaving no residual red puncta (Fig. 2*Cii*). When the same cells were subsequently imaged deeper within the cell, away from the cell membrane, by wide-field imaging (xenon lamp with 480/40 bandpass excitation filter), many fluorescent AO-labeled vesicles were observed (Fig. 2*Ciii*). All of these red fluorescent vesicles disappeared on 2 min of constant illumination (Fig. 2*Civ*). The release of the AO from these vesicles also occurred by a flash of fluorescence, which dissipated laterally in a manner similar to what we observed with TIR-FM (Fig. 2 *A* and *B*). Because the release occurred from AO-labeled vesicles that were not adjacent to the plasma membrane, this was the second observation inconsistent with the interpretation that AO flashes represent exocytosis.

A third observation inconsistent with exocytosis was that the AO released from the vesicles accumulated in the nuclei (Fig. 2*C*). Three cells exemplifying this are shown in Fig. 2*D*. It took <5 s to detect the first release of AO in the three cells (Fig. 2*E*, arrows). Within seconds of the first AO flash, the nuclear fluorescence began to increase and reached a plateau at which no AO-labeled vesicles were left in the cell. Thus, the AO was released into the cytosol, not outside of the cell. These results are consistent with photolysis and not with exocytosis.

To test whether photolysis of AO-labeled vesicles is specific to rat astrocytes, we repeated these experiments with cultured human (HeLa), canine (MDCK), hamster (CHO), and rat

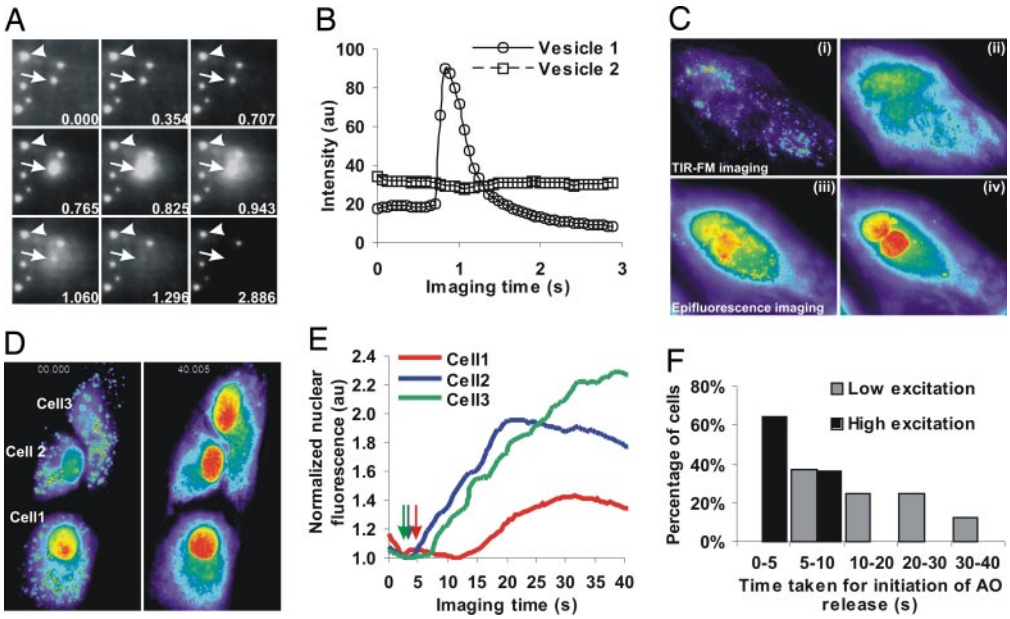

Fig. 2. Imaging fluorescently tagged vesicles in astrocytes. (*A*) Vesicles in a rat astrocyte labeled by using 5 μM AO, one of which did (arrow) and one that did not (arrowhead) release AO when imaged for 3 s by TIR-FM (530lp filter). (*B*) Quantification of fluorescence of the vesicles marked in *A* by an arrow (vesicle 1) and an arrowhead (vesicle 2). (*C*) Rat astrocyte labeled as above was imaged for 3 min by TIR-FM (530lp filter). (*i* and *ii*) Images show the cell at time 0 (*i*) and after 3 min of continuous laser exposure (*ii*). (*iii* and *iv*) Subsequently, the same cell was imaged continuously for 2 min by epifluorescence microscopy; images show the cell before (*iii*) and after (*iv*) epifluorescence imaging. The fluorescence intensity is pseudocolored red (highest) to violet (lowest). (*D*) A field of AO-labeled rat astrocytes was imaged continuously by epifluorescence microscopy (480/40 excitation filter and 530lp emission filter). The images show the cells at the first frame imaged (0 s) and 40 s after initiation of illumination. (*E*) A plot of nuclear fluorescence for each of these three cells starting from when the cells were first exposed to light. The colored arrows indicate the points at which the first AO flash was observed in each of these cells. (*F*) AO-labeled cells were imaged continuously by TIR-FM using a 488-nm laser at different intensities. The time at which the first AO flash was observed in each of at least 10 cells that were imaged with 1- and 10-mW laser illumination are plotted.

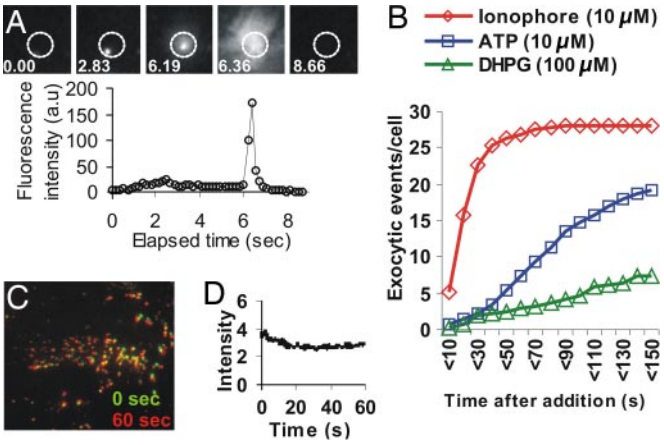

Fig. 3. Imaging lysosomal exocytosis using FITC-dextran. (*A*) Astrocytes whose lysosomes were loaded with FITC-dextran were imaged by TIR-FM. Images show a region where, after ionophore addition, a lysosome moved closer to the membrane and released the dextran. (*B*) The exocytosis of lysosomes, as assayed by FITC-dextran release in TIR-FM, was quantified after the addition of agents that raise cellular calcium (for each curve, $n > 5$). DHPG, (*R*,*S*)-3,5-dihydroxyphenylglycine. (*C*) Astrocytes whose lysosomes are labeled with 70-kDa FITC-dextran were imaged (525/50 bandpass emission filter) by TIR-FM under conditions similar to AO imaging. The overlay shows that all the vesicles present at the start of imaging (green) are also present after 60 seconds (red) of constant TIR-FM illumination. (*D*) Quantification of FITC-dextran fluorescence over time, of the imaging field in *C*.

(PC12) cells. For each of these cell types, the number and intensity of AO labeling was different, but illumination of the cells resulted in release of AO from the labeled vesicles (data not shown). When each of these cell types was incubated with lower concentration of AO, the vesicular labeling was weaker and it took longer for the AO fluorescence to be released from labeled vesicles. Similar results were observed in macaque (COS7) cells, which label very weakly with AO (data not shown). These results indicate that photolysis depends not only on the intensity of illumination but also on the concentration of AO in the vesicle.

Because AO accumulates in acidified organelles, these observations were limited to organelles, such as lysosomes and secretory vesicles. To test whether acidified organelles undergo photolysis even when not labeled with AO, we labeled the lysosomes with a different fluorescent marker, FITC-dextran. Previously, we have shown that lysosomes undergo Ca^{2+}-triggered exocytosis in a variety of cells (5). When astrocytes with FITC-dextran-labeled lysosomes were imaged as above for AO-labeled rat astrocytes after 1 min of continuous illumination with 2 mW of evanescent wave illumination, none of the FITC-dextran-labeled lysosomes released their contents (Fig. 3). The only change in FITC fluorescence was photobleaching over time. When astrocytes were treated with calcium ionophore to increase cytosolic Ca^{2+}, FITC-dextran was released from the lysosomes (Fig. 3*A*). Within a few seconds of ionophore addition, release from lysosomes (exocytosis) was initiated and continued to increase for 40 s (Fig. 3*B*). When astrocytes were treated with ATP (10 μM) and (*R*,*S*)-3,5-dihydroxyphenylglycine (100 μM), which raise cytosolic Ca^{2+} through cell surface receptor-mediated signaling, lysosomal exocytosis occurred but with a slower kinetics and to a lower extent than with ionophore (Fig. 3*B*). These results demonstrate that, under the labeling and imaging conditions used here, AO does, but FITC-dextran does not, induce vesicle photolysis. Thus, FITC-dextran is suitable for studying lysosomal exocytosis. We next tested whether other fluorescent weak bases, which also accumulate in lysosomes in high concentrations, would have similar effects. A number of fluorescent chemotherapeutic drugs, such as daunomycin and doxorubicin, are fluorescent and are known to accumulate in the acidified organelles (24). Furthermore, it has been proposed that sequestration into these organelles, and subsequent secretion through exocytosis, may be a mechanism for reducing the levels of these chemotherapeutics in the cytosol (26). When HeLa, MCF-7ADR, or NIH 3T3 fibroblasts were incubated with 2 μM doxorubicin or daunorubicin, the chemotherapeutics were observed in punctuate intracellular organelles (24). On illumination of the basal surface of the cell with TIR-FM, the chemotherapeutics were released from the vesicles in a series of flashes. However, on the basis of the criteria established above (the "released" drugs accumulated in the nucleus, and the flashes could be observed even in the middle of the cell), we determined that the release of these drugs was due to photolysis, not exocytosis (data not shown).

Next, we tested whether lysosomes in astrocytes do indeed undergo Ca^{2+}-triggered exocytosis. One approach to establish vesicle exocytosis is to monitor the delivery of its membrane cargo (lipid or integral membrane protein) to the cell membrane (27). On exocytosis, the fluorophores from the vesicle membrane should meet two criteria. First, the fluorophores should be fully delivered to the plasma membrane (none should be lost back into the cytoplasm). This is assayed by spatially integrating the fluorescence from a single vesicle. The total fluorescence should increase as the vesicle flattens, delivering its fluorophores to the membrane, which is deeper in the excitatory field. The fluorescence should stay high, as the fluorophores spread in the cell membrane, demonstrating that no fluorophores are lost back into the cell. Second, the fluorescence should spread laterally in the plane of the plasma membrane at a rate equal to the diffusion coefficient for that marker. This rate can be measured by measuring the slope of the increase in half-width^2 of the fluorescence with time (2, 27). We have previously used this approach to establish constitutive exocytosis of Golgi-derived and endocytic vesicles as well as Ca^{2+}-triggered exocytosis of lysosomes (2, 5, 28, 29).

To monitor Ca^{2+}-triggered lysosomal exocytosis, we labeled lysosomes with AO and with a fluorescently tagged lysosomal membrane protein CD63. When CD63-GFP is expressed in cells, it localizes to the lysosomal membrane, and on Ca^{2+}-triggered lysosomal exocytosis it gets delivered to the cell membrane (5, 30). When we increased the cytosolic Ca^{2+} of rat astrocytes with the calcium ionophore, A23187, fluorescent puncta of CD63-GFP were observed to disperse laterally in the plane of the plasma membrane (Fig. 4*A*). The peak fluorescence of the CD63-GFP (dashed line) increased, and then decreased. The total fluorescence (solid line) of the vesicle increased and remained high, which is consistent with delivery of all of the lysosomal membrane CD63 to the plasma membrane (Fig. 4*A′*).

The fate of the membrane marker CD63 was next examined in cells that had been incubated with AO. AO has a broad emission with two emission peaks (Fig. 1*B*), which are dependent on the dye concentration. At lower concentrations, the AO emission peak overlaps with green emitting fluorophores such as GFP, prohibiting simultaneous imaging of GFP and AO (31). Thus, to monitor the fate of CD63 in AO-labeled vesicles, we tagged CD63 with Cerulean (Cer), a bright photostable and monomeric variant of cyan fluorescent protein (32). The emission spectra of CD63-Cer did not overlap with AO, allowing simultaneous monitoring of the fate of AO in the vesicle lumen and CD63-Cer in the membrane. By using TIR-FM, we observed many vesicles for which the fluorescence of AO and CD63-Cer increased simultaneously, indicating that the vesicles approached the plasma membrane. In some of these vesicles, the peak and total fluorescence of the CD63-Cer and AO remained elevated (data not shown). This indicates that the vesicle approached, but did not release its contents. For some other vesicles, the peak and total intensities for AO rapidly decreased, whereas the fluorescence of the CD63-Cer remained constant

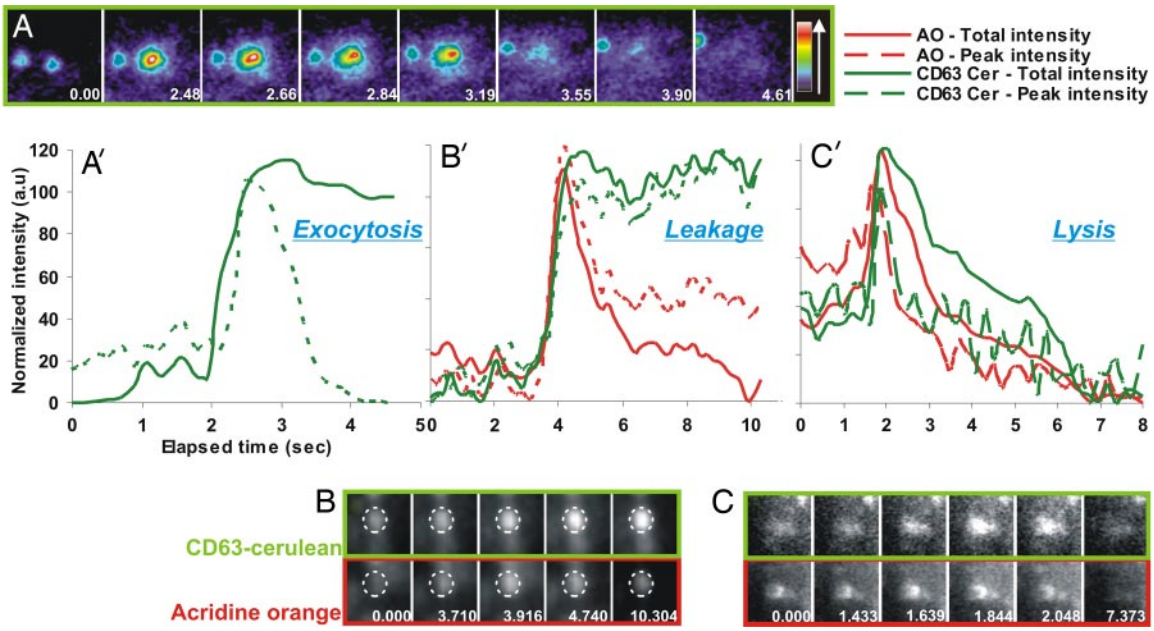

Fig. 4. Distinguishing vesicle fusion from leakage and lysis. (*A*) Rat astrocytes transiently transfected with CD63-GFP were imaged with TIR-FM. The images show a few selected frames from a movie of an exocytic vesicle before and after release of its membrane cargo CD63-GFP. The pixels are pseudocolored (scale on the right) to enable visualizing the lateral spread of CD63-GFP fluorescence. (*A′*) The changes in normalized peak and total intensity of this field are shown. (*B* and *C*) Simultaneous dual-color imaging of rat astrocytes transiently transfected with CD63-Cer (480/40 bandpass emission filter) and loaded with AO (580lp emission filter). (*B*) Images show a few frames from the movie of a vesicle (marked by circle) that undergoes photoinduced leakage. (*B′*) Quantification of AO (red) and CD63-Cer (green) fluorescence within the circle in *B*. (*C*) Images show photoinduced lysis of a vesicle, resulting in simultaneous loss of AO and CD63-Cer from the vesicle. (*C′*) The traces show total and peak intensities for the CD63-Cer (green) and AO (red) for vesicle shown in *C*. The number on each image is the time point at which it was taken and matches with the corresponding plot.

(Fig. 4 *B* and *B′*). This indicates release of AO from the vesicle with no delivery of the membrane protein CD63-Cer to the plasma membrane. Finally, we observed a class of vesicles where the peak intensities for AO and CD63-Cer increased simultaneously, and then decreased (Fig. 4*C*). However, the total intensity of the AO (solid red line) decreased slower than the peak intensity (dashed red line), and the total intensity of the CD63-Cer (solid green line) decreased even slower (Fig. 4*C′*). If the vesicle entered and then left the evanescent field, the intensities of the two fluorophores would have increased and decreased in parallel. Thus, the differential loss in fluorescence of CD63-Cer and AO indicates that it is not vesicle movement, but vesicle lysis followed by cytoplasmic diffusion of these markers at different rates. This is in contrast to what we observed for CD63 release in the absence of AO labeling (Fig. 4 *A* and *A′*).

Each of these behaviors was triggered by exposing cells to light; no agents that raise cytosolic Ca^{2+}, such as ionophore, were necessary. Previously, we have demonstrated that lysosomal exocytosis is Ca^{2+}-triggered (5). This, together with our present finding that lysosomes in rat astrocytes that are labeled with fluorescent dextran show no detectable basal exocytosis, offer additional evidence against the AO flash representing an exocytic event.

Discussion

Monitoring the dynamics of molecules during exocytosis is important for understanding many biological phenomena, such as neurotransmitter release at the neuronal synapse. Over the past few decades, there have been many significant advances in our knowledge of the molecules involved in this process (33). As a result of these studies, there is a greater focus on studying the activity of these molecules by characterizing their dynamics during exocytosis. These kinds of studies depend on assays that allow unambiguous identification and quantification of the steps of vesicle docking and fusion.

Because of the narrow plane of excitation that can be achieved along the cell surface, TIR-FM/evanescent wave microscopy provides high signal-to-noise ratio for imaging cell surface events (1, 34, 35). Thus, this approach is being used increasingly to monitor exocytosis of individual vesicles (27, 36). AO is a fluorescent weak base that can permeate the cell and vesicle membrane and, because of protonation, selectively accumulates in acidic compartments. Because the lumen of many secretory vesicles is acidic, AO readily labels them. Thus, AO was among the earliest fluorophores used to image vesicle exocytosis with TIR-FM (3). The bright flash, and subsequent lateral spread of AO fluorescence is considered "a hallmark of exocytosis," and it is used in many cell types for this purpose (3, 18, 20). Here, we used AO in an attempt to study Ca^{2+}-triggered vesicle exocytosis in rat astrocytes. However, a number of observations indicate that AO is not a suitable reporter for imaging exocytosis.

First, AO flashes occurred in all cells that were illuminated. The occurrence of AO flashes depended on the intensity of illumination and required no Ca^{2+} triggering. For this to be fusion, it would be necessary for the fusion machinery to be light- and/or temperature-sensitive. However, no fluorophore was released from the vesicles under identical laser excitation when the lumen was labeled with another fluorophore (FITC-dextran), or when a membrane protein on the same vesicle was tagged with GFP. This indicates that it is not an effect of laser illumination on the vesicle fusion machinery but on the AO that causes the release of the fluorophores from the vesicle.

Second, the time delay before initiation of AO flashes was decreased when AO in the vesicle was at lower concentrations. Thus, the photoinduced release of AO from vesicles depended on concentration of AO in the vesicle. This concentration-dependent release was not observed when the vesicles were

labeled with other fluorescent molecules, such as FITC-dextran or CD63-GFP, which are poor at photoinduced production of reactive oxygen. However, photoinduced release was observed with chemotherapeutics that can effectively generate reactive oxygen.

Third, the flash and lateral spread of the AO fluorescence was observed even when we focused the excitation light into the cytosol, micrometers away from the plasma membrane. Thus, the release of AO did not depend on the vesicle being tethered/docked or even in the vicinity of the plasma membrane.

Fourth, after the release of AO from the vesicle, the fluorescence never left the cell as would be expected of exocytosis. Instead, the fluorescence accumulated in the nucleus where AO binds to DNA. Our interpretation that the AO labeling induces photolysis is consistent with the reports in which excitation of AO-labeled purified lysosomes resulted in the release of lysosomal hydrolases (37).

And fifth, when AO was imaged simultaneously with a fluorescent membrane marker, even when the AO was released from the vesicle, the membrane protein was not delivered to the plasma membrane (Fig. 4 *B* and *C*). The CD63-Cer fluorescence associated with the vesicle increased as the vesicle approached the membrane (moving into the evanescent field) and then either stabilized (Fig. 4*B*) or diffused in the cytosol (Fig. 4*C′*) as the AO fluorescence rapidly decreased. In contrast, in the absence of AO, a vesicle labeled with CD63-GFP fused to the plasma membrane in a Ca^{2+}-dependent manner and the CD63-GFP was delivered to the plasma membrane (Fig. 4 *A* and *A′*).

These results have led us to the conclusion that all of the AO flashes we have observed are the result of vesicle lysis, not the fusion of vesicle to the plasma membrane. Recently, another independent study reported AO-induced vesicle photolysis when they used AO to label malignant melanoma cells (38). This study reported that, when the cells were treated with vacuolar H^+-ATPase inhibitor bafilomycin A1 before AO labeling, it resulted in no vesicles with red fluorescence and no AO flashes. This is in agreement with our results that cell lines that show reduced AO labeling also show fewer light-induced AO flashes. They also found that removal of oxygen from the media and the use of singlet oxygen scavengers, but not hydroxyl radical scavengers, reduced AO-dependent vesicle photolysis.

Our study raises two questions. First, can AO-triggered photolysis of vesicles be prevented? Inhibitors of the vacuolar ATPase block vesicle acidification and prevent vesicle lysis, but blocking acidification also prevents vesicle labeling with AO. Oxygen scavengers have been shown to prevent photolysis of AO-labeled vesicles (38, 39). This also indicates that excitation of AO generates singlet oxygen, which causes peroxidation of lipids in the vesicle membrane and leads to its lysis. However, use of agents to scavenge oxygen and prevent vesicle acidification would alter the cellular physiology and thus would not be recommended. We find that the latency as well as the extent of vesicle photolysis depends on the amount of AO in the vesicle and the intensity of illumination. Even when vesicles are loaded with less AO or when lower illumination intensities are used, it only delays (not prevents) photolysis (Fig. 2*F*). Thus, use of these approaches also requires distinguishing fusing vesicles from lysing vesicles. Moreover, because many of the variables, such as vesicle pH and hence extent of AO loading, that affect AO-induced photolysis are beyond experimental control, we believe that use of AO to image vesicle exocytosis should be avoided. If AO is used for monitoring exocytosis, in each instance it is essential to determine whether the AO flash is caused by vesicle lysis or exocytosis. The use of a marker that labels the vesicle membrane is a good means to achieve this distinction. There is spectral overlap of AO fluorescence with most of the commonly used fluorescent proteins, including GFP (31). Thus our demonstration that the CFP variant Cer can be used for such dual-color imaging applications offers a solution.

The second question that arises from our study is whether criteria can be established to unambiguously determine when exocytosis occurs. Our approach uses labels on the membrane components of the vesicle. For this, we have used the lysosomal membrane protein CD63 to examine Ca^{2+}-triggered lysosomal exocytosis in astrocytes. This allowed us to quantitatively distinguish between lysis and fusion of lysosomes as it met the following criteria. First, when the vesicle fuses to the plasma membrane, the fluorophores in the vesicle membrane should be delivered to the plasma membrane. Thus, if one quantifies the fluorescence of the vesicle membrane marker as the vesicle approaches and fuses to the membrane, the total fluorescence should increase, and stay constant, even as the peak fluorescence increases and then decreases (Fig. 4*A′*). In contrast, when the vesicle lyses, the total and peak fluorescence would increase and decrease rapidly (Fig. 4*C′*). Second, when the vesicle fuses, the membrane-bound fluorophores should spread laterally in the plane of the plasma membrane and the fluorescent area should increase linearly with time at a rate that is equal to the diffusion coefficient of the membrane probe. Previously, we have successfully applied this approach to demonstrate vesicle fusion by using fluorescent lipids and membrane proteins such as p75, neural cell adhesion molecule, Glut4, transferrin receptor, CD63, and vesicular stomatitis virus–glycoprotein (2, 4, 5, 28–30). Here, by using lysosomal membrane protein CD63 and AO labeling, we have demonstrated the various fates of the vesicle membrane marker as the vesicle undergoes fusion, leakage, or lysis.

In conclusion, the demonstration that AO labeling causes photolysis of vesicles raises questions about many of the previous studies that have relied on the use of AO release as a reporter for exocytosis without addressing the question of vesicle photolysis. Our approach of monitoring membrane marker together with the analysis discussed above offers a decisive assay to determine the fate of a vesicle labeled with AO or any other dye of interest. Use of the approach described here establishes that lysosomes undergo Ca^{2+}-triggered exocytosis in astrocytes. Future work is needed to address the physiological significance of Ca^{2+}-triggered lysosomal exocytosis for astrocytes.

Materials and Methods

Cell Culture and Treatment with AO and FITC-Dextran. Rat astrocytes were isolated as described in ref. 40 and grown in DMEM/F12 media supplemented with 10% FBS and 0.75% glucose (Sigma–Aldrich, St. Louis, MO) in 5% pCO_2 at 37°C. For imaging, cells were plated onto glass coverslips (Fisher Scientific, Pittsburgh, PA) or on glass-bottom dishes (MatTek, Ashland, MA) coated with 1% gelatin (Sigma–Aldrich) and imaged in OptiMEM (Invitrogen, Carlsbad, CA). Cells were transfected by using Lipofectamine 2000 (Invitrogen) and imaged 1–2 days after transfection. An aqueous stock solution of AO (10 mM; Molecular Probes, Eugene, OR) was diluted appropriately and added to the cell culture media to yield the desired concentration of 0.1–5 μM as mentioned. The cells were incubated in AO-containing media at 37°C for various times (up to 15 min) followed by three washes with PBS (Invitrogen) to remove AO not taken up by cells. FITC-dextran labeling of lysosomes was performed as described in ref. 5.

Microscopy and Data Analysis. Through-the-objective TIR-FM and epifluorescence microscopy were performed with an inverted Olympus IX-70 microscope with an APO ×60, N.A. 1.45 TIR objective (Olympus Scientific, Melville, NY) equipped with a 12-bit cooled CCD camera (ORCA-ER; Hamamatsu Photonics, Hamamatsu, Japan). The camera, the Mutech MV1500 image acquisition card (Mutech, Billerica, MA), and the mechanical shutters (Uniblitz; Vincent Associates, Rochester, NY) were

controlled by MetaMorph (Molecular Devices, Downingtown, PA). The microscope was enclosed in a home-built chamber for temperature control, and all imaging was performed at 37°C. For TIR-FM, FITC, GFP, and AO were excited with the 488-nm line of an air-cooled tunable argon laser (Omnichrome; model 543-AP A01; Melles Griot, Carlsbad, CA) reflected off a dichroic beamsplitter (z488rdc). For epifluorescence, the light of a xenon short-arc lamp [model UXL-150M0 (Ushio, Tokyo, Japan) in an OPTI QUIP (Highland Mills, NY) model 770 housing with power supply model 1600] was passed through a 480/40 bandpass excitation filter. The emitted fluorescence for both TIR-FM and epifluorescence microscopy was passed through appropriate emission filters (green channel, 515/30 or 525/50; red channel, 580lp or 600lp) as indicated for each experiment. Simultaneous dual-color TIR-FM imaging of Cer and AO was achieved by exciting Cer with a He–Cd laser (442-nm laser; Omnichrome 4056-S-A02 with LC-500 power supply) and AO with the 514-nm laser line of the tunable argon laser reflected off a z442/515rpc beamsplitter. The emission was spectrally separated by means of an emission splitter (DualView; Optical Insights, Santa Fe, NM) equipped with a 515/30 bandpass filter and a 580lp filter. All filters, dichroics, and polychroics were from Chroma Technologies (Brattleboro, VT). The depth of the evanescent field was usually 70–120 nm. Images containing a region of interest were streamed to memory during data acquisition and saved to hard disk afterward. Data analysis was performed by using MetaMorph software (Molecular Devices).

Emission Spectra. The emission spectra of AO at different concentrations were measured with a Tecan (Durham, NC) Safire plate reader with 442-nm excitation in 1-nm increments in sodium acetate buffer (Sigma–Aldrich) at pH 5.0.

We thank Jane Lin (New York Medical College, Valhalla, NY) for providing some of the cells and David Piston (Vanderbilt University Medical Center, Nashville, TN) for providing the Cerulean construct used in this study. We thank Katherine Heyman for help in editing this manuscript. This work was supported by National Science Foundation Research Grant BES-0620813 and National Institutes of Health Grant P20 GM072015.

1. Johns LM, Levitan ES, Shelden EA, Holz RW, Axelrod D (2001) *J Cell Biol* 153:177–190.
2. Schmoranzer J, Goulian M, Axelrod D, Simon SM (2000) *J Cell Biol* 149:23–32.
3. Steyer JA, Horstmann H, Almers W (1997) *Nature* 388:474–478.
4. Fix M, Melia TJ, Jaiswal JK, Rappoport JZ, You DQ, Sollner TH, Rothman JE, Simon SM (2004) *Proc Natl Acad Sci USA* 101:7311–7316.
5. Jaiswal JK, Andrews NW, Simon SM (2002) *J Cell Biol* 159:625–635.
6. Lang T, Wacker I, Steyer J, Kaether C, Wunderlich I, Soldati T, Gerdes HH, Almers W (1997) *Neuron* 18:857–863.
7. Reddy A, Caler EV, Andrews NW (2001) *Cell* 106:157–169.
8. Coorssen JR, Schmitt H, Almers W (1996) *EMBO J* 15:3787–3791.
9. Chavez RA, Miller SG, Moore HP (1996) *J Cell Biol* 133:1177–1191.
10. McNeil PL, Steinhardt RA (2003) *Annu Rev Cell Dev Biol* 19:697–731.
11. Stinchcombe J, Bossi G, Griffiths GM (2004) *Science* 305:55–59.
12. Nedergaard M, Ransom B, Goldman SA (2003) *Trends Neurosci* 26:523–530.
13. Ransom B, Behar T, Nedergaard M (2003) *Trends Neurosci* 26:520–522.
14. Seifert G, Schilling K, Steinhauser C (2006) *Nat Rev Neurosci* 7:194–206.
15. Montana V, Malarkey EB, Verderio C, Matteoli M, Parpura V (2006) *Glia* 54:700–715.
16. Zoccarato F, Cavallini L, Alexandre A (1999) *J Neurochem* 72:625–633.
17. Tsuboi T, Rutter GA (2003) *Curr Biol* 13:563–567.
18. Bezzi P, Gundersen V, Galbete JL, Seifert G, Steinhauser C, Pilati E, Volterra A (2004) *Nat Neurosci* 7:613–620.
19. Miedema H, Staal M, Prins HB (1996) *J Membr Biol* 152:159–167.
20. Tsuboi T, Zhao C, Terakawa S, Rutter GA (2000) *Curr Biol* 10:1307–1310.
21. Tsuboi T, Kikuta T, Sakurai T, Terakawa S (2002) *Biophys J* 83:172–183.
22. Avery J, Ellis DJ, Lang T, Holroyd P, Riedel D, Henderson RM, Edwardson JM, Jahn R (2000) *J Cell Biol* 148:317–324.
23. Zelenin AV (1993) in *Fluorescent and Luminescent Probes for Biological Activity*, ed Mason WT (Academic, San Diego), pp 83–99.
24. Altan N, Chen Y, Schindler M, Simon SM (1998) *J Exp Med* 187:1583–1598.
25. Taraska JW, Perrais D, Ohara-Imaizumi M, Nagamatsu S, Almers W (2003) *Proc Natl Acad Sci USA* 100:2070–2075.
26. Simon SM (1999) *Drug Discov Today* 4:32–38.
27. Jaiswal JK, Simon SM (2007) *Nat Chem Biol* 3:92–98.
28. Kreitzer G, Schmoranzer J, Low SH, Li X, Gan Y, Weimbs T, Simon SM, Rodriguez-Boulan E (2003) *Nat Cell Biol* 5:126–136.
29. Lampson MA, Schmoranzer J, Zeigerer A, Simon SM, McGraw TE (2001) *Mol Biol Cell* 12:3489–3501.
30. Jaiswal JK, Chakrabarti S, Andrews NW, Simon SM (2004) *PLoS Biol* 2:1224–1232.
31. Nadrigny F, Li D, Kemnitz K, Ropert N, Koulakoff A, Rudolph S, Vitali M, Giaume C, Kirchhoff F, Oheim M (2007) *Biophys J* 93:969–980.
32. Rizzo MA, Springer GH, Granada B, Piston DW (2004) *Nat Biotechnol* 22:445–449.
33. Jahn R, Lang T, Sudhof TC (2003) *Cell* 112:519–533.
34. Axelrod D (2001) *Traffic* 2:764–774.
35. Jaiswal JK, Simon SM (2003) in *Current Protocols in Cell Biology*, eds Bonifacino JS, Dasso M, Lippincott-Schwartz J, Harford JB, Yamada KM (Wiley, Hoboken, NJ), pp 4.12.1–4.12.15.
36. Steyer JA, Almers W (2001) *Nat Rev Mol Cell Biol* 2:268–275.
37. Zdolsek JM, Svensson I (1993) *Virchows Arch B Cell Pathol* 64:401–406.
38. Hiruma H, Katakura T, Takenami T, Igawa S, Kanoh M, Fujimura T, Kawakami T (2007) *J Photochem Photobiol B* 86:1–8.
39. Zdolsek JM, Olsson GM, Brunk UT (1990) *Photochem Photobiol* 51:67–76.
40. Takano T, Kang J, Jaiswal JK, Simon SM, Lin JH, Yu Y, Li Y, Yang J, Dienel G, Zielke HR, *et al.* (2005) *Proc Natl Acad Sci USA* 102:16466–16471.